

HYBRID JOINT CONTROL SYSTEM MODELLING

Vukobratović M., Hristić D. *)
Ivančević V. **)

- *) Robotics Laboratory, Mihailo Pupin Institute
Belgrade, YUGOSLAVIA
- **) Yugoslav Institute for Sports Medicine,
Belgrade, YUGOSLAVIA

ABSTRACT - A solution of one human extremity joint hybrid control is proposed. A joint with predominantly one degree of freedom was selected (elbow or knee). Basic energy, in principle a smaller part, is obtained by efferent electrical stimulation of the neuro-muscular plates of the natural actuator in the given joint. Simultaneously and constantly stimulation of both the m. agonist and m. antagonist of the desired movement is performed, whereby m. agonist is stimulated by Heaviside's rectangular input and m. antagonist by an exponential input. External energy is supplied by an electromechanical actuator, already realized for the active orthosis. The parameters of the engaged muscles were obtained at the basis of: Hill's hyperbolic relation of muscular contraction velocity and tension, Wilky's serial elastic element, Hodgkin-Huxley's law of impuls conduction through giant axons and synaptic electrochemical transmission. These relations serve simultaneously as basis of the internal control system being realized at muscular level in the form of Houk's autogenetic reflex (length and force muscle feedbacks). The control system contains some simplified form of the internal/external energy repartition. Simulation results for step, ramp and sinus inputs are given.

FES, Rehabilitation Robots, Active Orthosis, Hybrid Joint, Control.

INTRODUCTION

Functional Electrical Stimulation (FES), both in efferent and afferent mode, has been subject of intensive study and research in the course of the last 20 years or more. Encouraging results were obtained, some of them practically applied as in the case of the Peroneal Stimulator, although wider spread out notably in the case of more complex and prolonged motor activities were limited by two main factors:

- non-repeatable response of the stimulated muscles to FES,
- fast fatigue of muscle groups during prolonged activity.

The idea of the so-called "hybrid joint" is not a new one //1/. But, since this paper, some attempt to develop a hybrid

joint model and its control was not published. This present work presents the simulation results of a hybrid joint control system modelling, where stimulated muscles are supported by external power via an electromechanical orthotic drive.

EFFERENT FUNCTIONAL ELECTRICAL STIMULATION MODEL

The process of functional electrical stimulation (FES) provides or improves functional movements of an abnormal neuromuscular system by the application of electrical pulses to the efferent or afferent peripheral neural fibres. These pulses are supplied by either skin electrodes or implantable stimulators and are controlled by volitional control signals by the patient who thus regains, to some extent, voluntary control over his paretic muscle /2/.

One can use either efferent or afferent FES to attain functional movements. In efferent stimulation (EFES) the patient activates the stimulator with his volitional control signals (VCS) which excites the efferent nerves or muscle end plates and thus produces direct muscle contraction. According to Hatze /3/, the force developed by the single muscle contraction is equal to the product to the active state, the length-tension function and the velocity-tension function of the muscle.

According to /4/ the active state $q: R_{exc} \rightarrow R_{resp}$ can be represented by the following first order differential equation

$$\dot{q} + cq = cQA, \quad 0 \leq Q \leq 1, \quad (1)$$

where A denotes the maximum tension a single muscle can develop, while $Q = Q(r)$ is the "desired" active state as a function of input stimulus rate r. In the limiting case $Q = 1$ and input of the active state remains proportional to the maximum tension. Also, in the relative muscle length interval $1 < L \leq 1.125$ the length-tension function is equal to /4/, as well as the velocity-tension ratio F/F_0 (where $F = F(x)$ and $F_0 = \max(F)$) is equal to 1 in the maximum limiting case.

Exponential curve $q: R_{exc} \rightarrow R_{resp}$ (a solution of equation (1)) is already capable of representing the most simple and executive EFES model, for its global behaviour agreement with average empirical force-time curves were obtained both "in vitro" and "in vivo" /5/. But some in-depth analysis of the curve itself suggests an existence of inflexion somewhere around the start of contraction, while classical mechanics of contraction requires inclusion of the known Hill's "characteristic" force-velocity relation /6/ into any macroscopic muscle model. Wilkie's variant of this basic relation /7/, describing both contractile and series elastic component behaviour of the shortening muscle can be stated as

$$\dot{x} = \frac{b^*(F_0 - F)}{F + a^*} - \frac{d}{dt}(c \cdot x) \quad (2)$$

where: a^* corresponds to energy dissipated during the contraction, b^* is phosphagenic energy transducing rate /6/, while c denotes

an elastic constant. These constants can be put into the dimensionless form by the use of fractions

$$a = a^*/F_0, \quad b = b^*/x_0, \quad \dot{x}_0 = F_0/(a^*b^*) \quad (3)$$

The synaptic FM/AM modulation of the EFES signal, playing the role of input transducer to the contraction, can be presented by function of the mediator (e.g. acetylcholine or noradrenaline or serotonin) amount $d:R^{trans} \rightarrow R^{receiv}$ on the actual neuro-muscular connection (end plate) /8/.

Finally, the EFES signal transmission through efferent nerves should satisfy the known Hodgkin-Huxley's law of impulse conduction $Q:R^{trans} \rightarrow R^{trans}$ /9/ taking the Heaviside's excitation form

$$Q = Q_0(h(t) - h(t-\tau)), \quad h(t-\tau) = \begin{cases} 0, & t-\tau < 0 \\ 1, & t-\tau > 0 \end{cases} \quad (4)$$

Now, the EFES-response mapping of skeletal muscle can be stated in the form of the force generator

$$F:R_t \rightarrow Hom_R(S, C), \quad T^2F + 2aT\dot{F} + cF = b\dot{Q}, \quad (5)$$

where: t denotes stimulation time, S and C correspond to the left R -moduli of stimulation and contraction respectively, T is muscle time characteristics. As the condition $a^2 > c$ is naturally fulfilled for skeletal muscles, the response has exactly the desired aperiodic form, completely agreeing with the empirical curves /5/, as presented in Figure 1.

THE HYBRID SYSTEM MODEL

The EFES orthosis for the pair of mutually antagonistic muscles is combined with external power drive into a hybrid joint orthosis (Fig. 2).

a) External actuator

A d.c. servo motor "DUOPERM SUPER" is used as an external actuator, according to differential equations /10/

$$L_r \dot{i}_r + R_r i_r + C_E \dot{q} = u_r, \quad -C_M \dot{i}_r + J_r \ddot{q} + B_C \dot{q} = -\mu, \quad (6)$$

where is used: L_r - rotor inductance, R_r - rotor resistance, i_r - rotor current, q - angular position of the output shaft, u_r - rotor input voltage, C_E - electromotive force proportionality constant, C_M - torque proportionality constant, J_r - output shaft moment of inertia, B_C - output shaft viscous friction and μ - the motor external loading torque. Constant $I = 1/100$ denotes proportionality between an intersegmental - joint angle and the motor shaft.

b) Equation of motion

Newton equation of rotational joint motion $\delta = f(\theta, \dot{\theta}, t)$, representing an orthogonal uniaxial mapping $f:R_\theta \times R_{\dot{\theta}} \rightarrow R_t \times R_\delta$ (where θ denotes the actual joint angle) is proposed in the linear

viscoelastic form

$$J\ddot{\theta} + B\dot{\theta} + C\theta = \sum_{k=1}^2 \sigma_k (F_k \cdot r_k - mgh \sin \theta) + \mu(t - T_\mu), \quad (7)$$

where is used: J - combined moment of inertia of the actual human body segment and motor output shaft, B - combined viscous friction of the actual joint tendon and motor output shaft, C - tendon elasticity coefficient, $\sigma = 1$ ($k=1$) for agonistic (i.e. flexor) muscle and $\sigma = -1$ ($k=2$) for antagonistic (extensor) one, $F = F(t)$ - actual muscle force (5), $r = r(\theta)$ - joint level arm of the actual muscle tendon, h - the actual segment length and T_μ - the motor torque time lag constant, corresponding to 70% of F_{\max} .

c) The state equation

The total system model, including equation of motion (7), two antagonistic muscle force FES generators (5) and external power actuator (6) could be put into the canonical form by the use of substitutions: $x_1 = \theta$, $x_2 = \dot{\theta}$, $x_3 = F_1$, $x_4 = \dot{F}_1$, $x_5 = F_2$, $x_6 = \dot{F}_2$, $x_7 = i_r$, $u_1 = Q_1$, $u_2 = Q_2$, $u_3 = u_r$. Now we have the seventh order system

$$\begin{aligned} \dot{x}_1 &= x_2 \\ \dot{x}_2 &= \frac{1}{J}(Cx_1 - Bx_2 - r_1 x_3 + r_2 x_5) + \frac{1}{J}(C_M \cdot Ix_2(t - T_\mu) - mgh \sin x_1) \\ \dot{x}_3 &= x_4 \\ \dot{x}_4 &= \frac{1}{T_1}(-c_1 x_3 - 2a_1 T_1 x_4) + \frac{1}{T_1}(b_1 u_1) \\ \dot{x}_5 &= x_6 \\ \dot{x}_6 &= \frac{1}{T_2}(-c_2 x_5 - 2a_2 T_2 x_6) + \frac{1}{T_2}(b_2 u_2) \\ \dot{x}_7 &= \frac{1}{L_r}(-C_E \cdot Ix_2 - R_r x_7) + \frac{1}{L_r}(u_3) \end{aligned} \quad (8)$$

$$\dot{x}^i = A_j^i x^j + B_k^i u^k + f^i, \quad (i, j=1, \dots, 7; k=1, 2, 3) \quad (9)$$

where x^i denotes state vector, u^k - scalar input vector, while system matrix A_j^i , input distribution matrix B_k^i and vector of nonlinear driving torques and loadings f^i are respectively defined with

$$A = \begin{pmatrix} 0 & 1 & 0 & 0 & 0 & 0 & 0 \\ -\frac{C}{J} & -\frac{B}{J} & \frac{r_1}{J} & 0 & -\frac{r_2}{J} & 0 & 0 \\ 0 & & & & & & \\ 0 & & & & & & 0 \\ 0 & 0 & 0 & 0 & -\frac{c_2}{T_2} & -\frac{2a_2}{T_2} & 0 \\ 0 & -\frac{C_E I}{L_R} & 0 & 0 & 0 & 0 & -\frac{R_F}{L_R} \end{pmatrix}$$

$$B = \begin{pmatrix} 0 & 0 & 0 \\ 0 & 0 & 0 \\ 0 & 0 & 0 \\ \frac{b_1}{T_1} & 0 & 0 \\ 0 & 0 & 0 \\ 0 & \frac{b_2}{T_2} & 0 \\ 0 & 0 & \frac{1}{L_R} \end{pmatrix}, \quad f = \begin{pmatrix} 0 \\ \frac{1}{J}(C_M I x_7(t-T) - mgh \sin x_1) \\ 0 \\ 0 \\ 0 \\ 0 \\ 0 \end{pmatrix} \quad (10)$$

The numerical values of the parameters are selected as follows:

- | | | | | | |
|--------------|----------------|--------------|---------------|--------------|--------------|
| $J = 0.1$ | $B = 0.8$ | $C = 0.1$ | $r_1 = 0.02$ | $r_2 = 0.02$ | $a_1 = 1.2$ |
| $a_2 = 1.2$ | $b_1 = 0.08$ | $b_2 = 0.08$ | $c_1 = 1.25$ | $c_2 = 1.25$ | $T_1 = 0.15$ |
| $T_2 = 0.15$ | $L_R = 0.0056$ | $R_F = 3.4$ | $C_E = 0.055$ | $C_M = 0.03$ | $I = 100$ |
| $T_M = 1.0$ | $m = 3.2$ | $g = 9.81$ | $h = 0.3$ | | |

THE HYBRID SYSTEM CONTROL

a) External control

The external control of the joint movement can be presented in the form /10/:

$$u = u_{\text{nom}}(t) + u(\theta, \dot{\theta}) \quad (11)$$

where $u_{\text{nom}}(t) = \theta(t)$ denotes the nominal programmed input realizing the pure externally driven functional movement in the joint under ideal conditions without perturbations and errors in initial conditions, while $u(\theta, \dot{\theta})$ denote goniometric position and velocity feedbacks, controlling the final (hybrid) movement realisation.

b) Neural control

Neural control is represented by length and force muscle feedbacks (see Figure 3) corresponding to Houk's autogenetic reflexes /11/. Here SP denotes muscle spindle (stretch receptor), TO - Golgy's tendon organs (force receptor), F - force measured by TO (equal to the sum of the test fibers response P and remaining fibers response D), C is series compliance, R - background excitatory level, E - efferent signal, H, G - gains of TO and SP respectively. The impulse stretch of the agonistic muscle (its length is obtained by the Wilkie's relation (2)) naturally produces the gain G, and in EFES is realized by an instantaneous increase of the stimulus rate r, producing the higher input Q_0 . On the other hand, overcoming of certain (individual) threshold level of the maximal realized force F_0 causes the decrease of EFES, analogously to the Golgy's reflex.

c) Biochemical control

According to /13/ the biochemical status of the biopsy samples from m. quadriceps femoris, taken during electrical stimulation at 20 Hz can be presented by diagram in Figure 4. The transducer of chemical energy to mechanical work in muscle is adenosine-triphosphate (ATP). The ATP store is in itself very limited and has to be continuously resynthesized. The sources for ATP resynthesis are breakdown of phosphocreatine (PCr) and glycolysis and, if oxygen is available, oxidative phosphorylation in mitochondria with pyruvate or fat acids as substrates. During maintained activation of a muscle there is a progressive decline in tension which is usually termed fatigue. It is not known what causes the decline in tension, though many theories prevail. Wilkie et al. /13/ were able to show, by the use of nuclear magnetic resonance technique, a close correspondence between reduction of ATP turnover rate and force decline during prolonged contractions. They also found a close correlation between force decline and increases in the hydrogen ion concentration.

Now, as a natural sensor of muscle fatigue, certain PH-meter ("Beckman Instr." or any of the similar kind) can be used by implantation. When the lactate content (see Fig. 4) approaches some critical value (about 50 seconds from the start of the continuous stimulated contraction), it means that PCr content approaches zero and the muscle is not any more capable of generating the force.

Therefore, the external power drive should be included into the movement approximately about 20 seconds from its start (which agrees with the intersection point of lactate and PCr curves) for the sake of the fatigue appearance delay. On the other hand, when the system is applied to some prolonged repetitive work (like walking), both the EFES and the external power drive inclusion should be coordinates such that the muscle work intensity would not exceed the so called moderate working zone /14/ in order to prevent great O_2 uptake and lacticacid accumulation in the working muscle.

The total hybrid system control can be presented as in Fig. 5.

A NOTE ON CONFIGURATIONAL GENERALIZATIONS

The presented hybrid model of a single joint is capable of some configurational generalizations by the use of certain differential geometry and topology techniques. In other words the general model of anthropomorphic active mechanism dynamics /15/

$$H(\theta)\ddot{\theta} + h(\theta, \dot{\theta}) = \mu, \quad H(\theta):R^n \rightarrow R^{n \times n}, \quad h(\theta, \dot{\theta}):R^n \times R^n \rightarrow R^n \quad (12)$$

can take some explicit configurational manifold interpretations, as follows.

Equation of motion (7) can be (at least theoretically) generalized to m joints, i.e. $(m+1)$ -segmental kinematic chain with the last segment being fixed. Its local coordinate description requires $6m$ Euclidean coordinates $x^r \in R^{6m}$. Including k holonomic constraints, we state the mapping $\theta:R^{6m} \rightarrow V^{6m-k}$, $\theta^i = \theta^i(x^r)$, $d\theta^i = \frac{\partial \theta^i}{\partial x^r} dx^r$ onto the Riemannian configurational manifold V^{6m-k} with the positively-definite metric form (kinetic energy like)

$$ds^2 = a_{ij} d\theta^i d\theta^j, \quad (i, j=1, \dots, 6m-k) \quad (\text{summation convention}) \quad (13)$$

The configurational metric tensor a_{ij} includes all inertial characteristics of the mechanism, given by

$$a_{ij} = \sum_{k=1}^m m(k) \delta_{rs} \frac{\partial x^r}{\partial \theta^i} \frac{\partial x^s}{\partial \theta^j}, \quad (\delta_{rs} - \text{Kronecker delta}, \quad (14) \\ r, s=1, \dots, 6m)$$

Substituting the segmental masses m in last relation by linear elasticity c and viscosity b coefficients of included joint constraints, we obtain respectively elastic and viscous tensors of the mechanism.

Now, the covariant generalization of a single joint equation of motion (7) can be stated in the linear form of local coordinates

$$a_{ij} \left(\frac{D^2 \theta^i}{Dt^2} + G^i \right) + b_{ij} \dot{\theta}^i + c_{ij} \theta^i = Q_j \quad (15)$$

Here, $Q_i = \sigma_k (F \cdot r)_i^k + \mu_i$, $G^i = (g \cdot \sin \theta)^i$,

$$\frac{D^2 \theta^i}{Dt^2} = \ddot{\theta}^i + \Gamma_{jk}^i \dot{\theta}^j \dot{\theta}^k, \quad (16)$$

and Γ_{jk}^i denote affine connections between R^{6m-k} and V^{6m-k} .

The configurational manifold V^{6m-k} globally presents topological product

$$V^{6m-k} = \prod_{i=1}^{6m-k} S^1_{(i)} = \{\theta^i: \text{mod } 2\pi\} \simeq R^{6m-k}/Z^{6m-k}, \quad (17)$$

(where Z denotes the set of integers), and this is exactly a $(6m-k)$ -dimensional torus T^{6m-k} .

Optimal trajectories of the mechanism motion are represented by geodesic lines on the torus T^{6m-k} , defined by: $\frac{D^2 \theta^i}{Dt^2} = 0$.

Now, the Tychonoff product theorem states that for such obtained topological space exists a "selector" A^{6m-k} , such that their quotient models are homeomorphic: $T^{6m-k}/\sim \approx A^{6m-k}/\sim$ (where " \sim " denotes an equivalent decomposition). And A represents a $(6m-k)$ -dimensional cub, defining the most natural command space for any active mechanism. Therefore, any set of the mechanism degrees of freedom has its simple, rectangular image in the command space "selector". For example, the command space for the two-degrees-of-freedom-mechanism is presented in Figure 6.

Simulation results are presented in Figs. 7-12.

GENERAL REMARKS: Simulation was performed in elbow joint. Time is measured in seconds (total = 2s), joint angle in radians and joint angular velocity in radians per second. In all figures, a) denotes time history of joint angle and b) denotes time history of joint angular velocity. In all simulations, zero initial conditions for all state variables as well as zero inputs have been used. Therefore arm was in resting elbow extension at the start of movement. In all simulations agonistic (flexor) muscle (m. biceps brachii) was stimulated by input ramp signal of $(10-t)$ Volts while the antagonistic one had a ramp input of $3(t-T)$ Volts. Here $T=1$ s denotes the moment of external power application.

- Fig. 7. Represents step input control with insufficient voltage.
- Fig. 8. Represents "optimal" step input controlled movement.
- Fig. 9. Represents ramp input control with insufficient voltage.
- Fig. 10. Represents "optimal" ramp input controlled movement.
- Fig. 11. Represents sinus input control with insufficient voltage.
- Fig. 12. Represents "optimal" sinus input controlled movement.

CONCLUSION

In the present study, a mathematical model for a single joint hybrid control system is given in a form of a quasi-linear seventh order state equation. It includes a one-degree-of-freedom equation of joint motion, two antagonistic muscle models of the second order and a well known external actuator model. The set of biological parameters is chosen to be inside the range of corresponding reference data. Experimental estimation of model parameters should be possible with more experiments, although the identification problem is difficult. It is believed that the proposed model appears to be the first step in hybrid control theory of human extremities and its biomechanical and orthotic applications.

The model is used for an elbow joint motion simulation. Obtained results show the following model characteristics: a) without the external control application the model is capable of performing approximately one third of a full-range joint motion, b) the model is "normally" sensitive to the external control changes, both in quantity and in shape, c) the hybrid system is completely capable of performing the full-range single joint motion with various angular velocities.

Finally, the presented model can be easily generalized to more-segmental configurations of the human body motion, and also technically realized as a powerful orthotic device, for the sake of its linear components.

REFERENCES

- /1/ Vukobratović M. (1973), How to control artificial anthropomorphic systems, IEEE Trans. on Systems, Man and Cybernetics, 5: 497-507.
- /2/ Vodovnik L., Kralj A. and Bajd T. (1985), Modification of abnormal motor control with functional electrical stimulation of peripheral nerves. In: Recent achievements in restorative neurology 1 (eds. Eccles, Dimitrijevic, Karger, Basel.
- /3/ Hatze H. (1978), A general myocybernetic control model of skeletal muscle. Biol. Cybern., 28: 143-157.
- /4/ Zheng Y.F., Hemami H. and Stokes B.T. (1984), Muscle dynamics, size principle and stability. IEEE Trans. Biomed. Engg., 31: 489-497.
- /5/ Viitasalo J.T. and Komi P.V. (1978), Force-time characteristics and fiber composition in human leg extensor muscles. Eur. J. Appl. Physiol., 40: 7-15.
- /6/ Hill A.V. (1938), Heat of shortening and the dynamic constants of muscle. Proc. Roy. Soc., (London), B, 126: 136-195.
- /7/ Wilkie D.R. (1950), The relation between force and velocity in human muscle. J. Physiol., 110: 249-280.
- /8/ Hoyle G., Castillo J. (1979), Neuromuscular transmission in Peripatus. J. Exp. Biol., 83: 13-29.
- /9/ Hodgkin, A., Huxley A. (1952), A quantitative description of membrane current and its application to conduction and excitation in nerve. J. Physiol. (London), 117: 500-544.
- /10/ Vukobratović M., Stokić D., (1982), Control of manipulation Robots, Springer-Verlag, Heidelberg, London, New-York, Tokyo.
- /11/ Houk J.C. (1979), Regulation of stiffness by skeletomotor reflexes. Ann. Rev. Physiol., 41: 99-114.
- /12/ Hultman E. and Sjöholm H. (1983), Energy metabolism and contraction force of human skeletal muscle "in situ" during electrical stimulation. J. Physiol. (London), 345: 525-532.
- /13/ Dawson M.J., Gadian D.G. and Wilkie D.R. (1978), Muscular fatigue investigated by phosphorus nuclear magnetic resonance. Nature, 274: 861-865.
- /14/ Chaffin D.B. (1973), Localized muscle fatigue-definition and measurement. J. Occup. Med. 15: 346-354.
- /15/ Vukobratović M., (1975), Legged Locomotion Robot and Anthropomorphic Mechanisms, Mihailo Pupin Institute, Beograd.

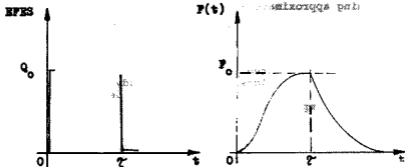


Fig.1 Heaviside's excitation and muscle response

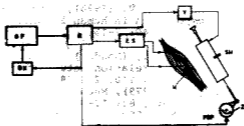


Fig.2 Joint orthosis with hybrid system; ref./1/, 1973.



Fig.3 Length and force muscle feedbacks

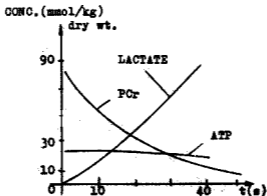


Fig.4 Biochemical status of stimulated muscle

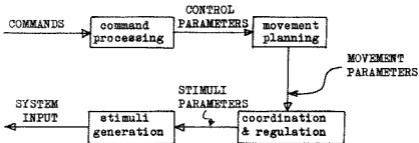


Fig.5 Processing framework of hybrid orthosis

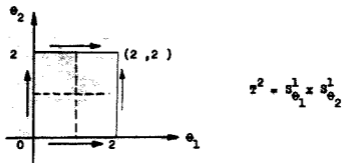
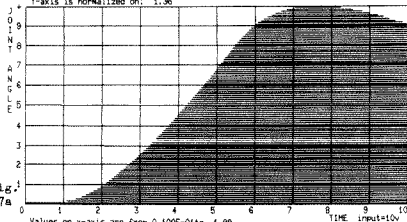
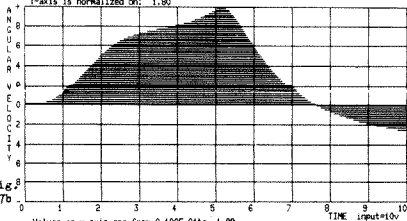


Fig.6 Command space - "selector" of the 2-nd order

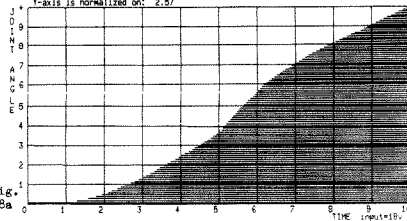
Values on x-axis are from 0.100E-01 to 1.99
 Y-axis is normalized on: 1.36



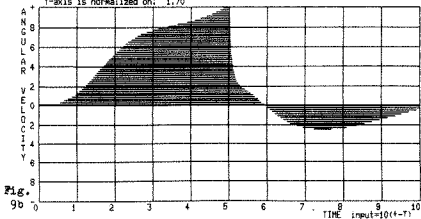
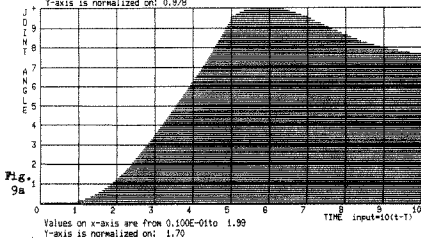
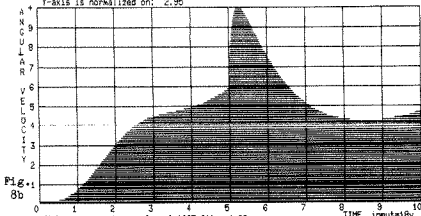
Values on x-axis are from 0.100E-01 to 1.99
 Y-axis is normalized on: 1.80



Values on x-axis are from 0.100E-01 to 1.99
 Y-axis is normalized on: 2.57



Values on x-axis are from 0.100E-01 to 1.99
Y-axis is normalized on: 2.95



Values on x-axis are from 0.100E-01 to 1.0
 Y-axis is normalized on: 1.31

